Electric-field effects on H^- photodetachment with excitation of $H(n = 2)$

Ning-Yi Du, Ilya I. Fabrikant, and Anthony F. Starace
Department of Physics and Astronomy, University of Nebraska, Lincoln, Nebraska 68588-0111
(Received 10 June 1993)

A theory of the photodetachment of hydrogen negative ions in an external static electric field with the production of hydrogen in excited states is developed. We use a combination of the frame-transformation theory and the Green's-function method. The cross section in nonzero fields is expressed in terms of the photodetachment matrix elements for zero field. The latter are calculated using the adiabatic hyperspherical representation. For energies close to the threshold we use a smooth extrapolation of the zero-field photodetachment matrix elements down to threshold taking care to enforce the proper threshold behavior of cross sections for nonzero fields. The ripples in the *total* cross section due to interference effects are not noticeable for incident photons linearly polarized along the static field direction, but are relatively well pronounced for the case of circularly polarized photons propagating along the static field. On the other hand, all *partial* cross sections corresponding to photodetached electrons having magnetic quantum number $m'=0$ (with respect to a quantization axis parallel to the static electric field) show significant ripple structure regardless of the light polarization. The partial cross section for detachment with excitation of the $n=2$, $m=1$ Stark substate by circularly polarized photons exhibits a particularly distinct ripple structure. All cross sections in the region of the shape resonance increase with increasing electric field in accordance with experimental observations. This effect is stronger in the case of linear polarization. We also predict a fairly stable value for the width of the $^1P^o$ shape resonance as a function of the electric-field strength over the range from 0.4 to 1 MV/cm. For electric-field strengths below 0.4 MV/cm, the ripple structure in the shape resonance makes it difficult to define a resonance width.

PACS number(s): 32.80.Fb, 32.60.+i

I. INTRODUCTION

Investigation of the behavior of negative ions in external fields gives important information about atomic structure and about the interactions between electrons and atoms [1]. Some effects demonstrate interesting phenomena illustrative of basic quantum mechanics. A typical example is the prediction [2] and observation [3] of interference effects in one-photon detachment of negative ions in a static electric field. Various combinations of external fields (namely, laser fields, and static electric and magnetic fields) allow one to control atomic processes involving negative ions.

An interesting aspect of the problem is the influence of external electric fields on resonances. Variation of resonance widths with electric-field strength was observed experimentally in photodetachment of H^- [4–7]. These experiments studied the Stark splitting of the Feshbach resonances below the $n=2$ excitation threshold as well as the shape resonance above the $n = 2$ threshold. Theoretical calculations [8–10] based on discrete-state atomic-structure methods have been able to describe some of the observed features. However, these methods are not able to calculate the photodetachment cross sections. Most scattering calculations incorporating the proper boundary conditions deal only with the short-range interaction between the escaping electron and the atomic residue (see, e.g., [11–14]), ignoring the long-range dipole and polarization interaction of the detached electron with the residual atom. Only recently have results for photodetachment of the H^- ion near the $n=2$ excitation threshold been obtained by Slonim and Greene [15]. These authors were mostly concerned with the behavior of the Feshbach resonance in the presence of the field and treated the above-threshold cross section at only a single electric field value $F=255$ kV/cm.

In this paper we present more detailed results for one-photon detachment of H^- with excitation of $H(n = 2)$ in the presence of both a static electric field and the long-range, final-state dipole interaction. This latter interaction occurs when the electron escapes from the H^- ion leaving the H atom in an excited state. Three aspects of the problem of detachment in an electric field are of interest. The first aspect is the interference effect [2], which can cause a ripple structure in the photodetachment cross section above the $n=2$ threshold. The second aspect is the effect of the electric field on the well-known $^1P^o$ shape resonance above the $H(n = 2)$ threshold.

The third aspect is the rescattering effect, i.e., the scattering by the residual atom of the detached electron wave reflected by the electric field's potential barrier. This effect was shown to be small if the electron leaves atomic hydrogen in its ground state [14]. However, if the final atomic state is excited, the effect may be much stronger due to the long-range dipole interaction. In the energy range for which $k^3 > F$ (in a.u.), where k is the final-state electron wave number, a simple representation for the photodetachment matrix element has been obtained

[16] which includes the photodetachment matrix element in the absence of the electric field and transition amplitudes describing scattering by the excited states. In the present paper we generalize these expressions and perform calculations employing the photodetachment matrix elements obtained within the adiabatic hyperspherical representation. The adiabatic hyperspherical approach [17] incorporates many of the electron correlations that are important in H^-. It has been successfully used for the calculations of one- and two-photon detachment in zero static field [18,19]. In addition, near-threshold resonant structure can be interpreted in terms of the adiabatic hyperspherical potentials of this system [20]. Furthermore, the hyperspherical representation describes correctly the effects of the long-range dipole interaction.

II. THEORY

A. Overview

Our general approach is to relate wave functions for the H($n = 2$)-e^- three-body Coulomb system calculated in zero electric field to wave functions appropriate for electron motion in the external electric field. We do so by means of an appropriate frame transformation. Such a frame-transformation theory was suggested by Fano [21] and Harmin [22] for photoionization in an electric field. It was developed for photodetachment in external magnetic [23] and electric fields [11,24] by Greene, Rau, and Wong. The key idea is that there are essentially three important regions of space for such processes [24]: (I) an inner region near r=0 where electron-atom interactions are dominant and which are best described in coordinates appropriate for the atom; (II) an intermediate region in which the detached electron does not have significant interaction with either the atom or with the external field and which thus may be described either in coordinates appropriate for the atom or in a coordinate system appropriate for the external field (e.g., cylindrical coordinates); and (III) a far region in which the electron is strongly influenced by the external field and which is best described in coordinates appropriate for the external field.

In the present work the following procedure is employed. Dipole transitions are computed in region I in hyperspherical coordinates using the adiabatic hyperspherical approximation for the H($n = 2$)-e^- system [18]. This approximation permits treatment of many of the important electron correlations as well as the long-range dipole field interaction between the degenerate H($2s, 2p$) states and the detached electron. In region II the hyperspherical final-state wave functions are transformed to an independent electron basis. The detached electron's wave function is then expanded in cylindrical coordinates, which are appropriate for matching it in region III to a field-dependent wave function for the detached electron. In order to take into account the proper boundary conditions for the detached electron, we perform this matching using the multichannel Green's-function approach developed in Ref. [16]. Our approach differs from that of Refs. [21–24] in that the many-body interactions in region I are treated here by *ab initio* theoretical calculations rather than semiempirically by means of quantum-defect theory.

A unique feature of the present calculations is the treatment of photodetachment plus excitation. For the H atom, of course, the excited states are degenerate. In the presence of the external field, however, the splitting of this degeneracy must be taken into account. This requires an additional frame transformation: the one from the nlm representation of the H atom to that of the Stark states of the H atom.

B. Formulation

We characterize the final state of the H($n = 2$)-e^- system by its total energy E, a set of quantum numbers b specifying a particular atomic final state, and the component m' of the detached electron's angular momentum along the electric field, which defines the z axis. The final-state wave function, normalized to a δ-function of energy E, is therefore denoted by $\Psi^-_{bm'E}$. The relation between E and the detached electron's energy $k_b^2/2$ is given by conservation of energy:

$$E \equiv E_i + \hbar\omega = E_b + \frac{1}{2}k_b^2. \tag{1}$$

Here E_i is the energy of the initial negative-ion state, $\hbar\omega$ is the photon energy, and E_b is the energy of the final atomic state. For our purposes it will be necessary to express the function $\Psi^-_{bm'E}$ in terms of the zero-field functions in spherical coordinates using a frame transformation. In order to develop such a transformation, we examine first the Lippman-Schwinger representation for $\Psi^-_{bm'E}$.

1. *Lippman-Schwinger equation for* $\Psi^-_{bm'E}$

Following the approach of Ref. [16], we expand the final-state function $\Psi^-_{bm'E}$ in the wave functions $\Phi_a(\mathbf{r}_A)$ of the atomic Hamiltonian,

$$\Psi^-_{bm'E}(q, \mathbf{r}_A, \mathbf{r}) = \mathcal{A}\sum_a \Phi_a(\mathbf{r}_A)\psi^-_{abm'E}(q, \mathbf{r}), \tag{2}$$

where $\mathcal{A}$ stands for the antisymmetrization operator and where $q^2/2$ is the longitudinal energy of the detached electron and $(k_b^2 - q^2)/2$ is the transverse energy of the detached electron.

The functions $\psi^-_{abEm'}$ satisfy a system of Lippman-Schwinger close-coupling equations,

$$\psi^-_{abm'E}(q, \mathbf{r}) = \delta_{ab}\psi^{(0)}_{bm'E}(q, \mathbf{r}) - \sum_c \int G^-_{aE}(\mathbf{r}, \mathbf{r}')U_{ac}(\mathbf{r}')\psi_{cbm'E}(q, \mathbf{r}')d\mathbf{r}', \tag{3}$$

where $\psi^{(0)}_{bm'E}$ is the electron wave function in the channel b in the absence of the electron-atom interaction (i.e.,

$\psi^{(0)}_{bm'E}$ represents an electron moving in the electric field), G^-_{aE} is the Green's function for the electron motion in the external field in channel a, and U_{ac} is the matrix element for the electron-atom interaction.

The exact expression for the function $\psi^{(0)}_{bm'E}$ is well known [11,14]:

$$\psi^{(0)}_{bm'E}(q,\mathbf{r}) = \frac{2^{1/3}e^{im'\phi}}{(2\pi)^{1/2}F^{1/6}}\mathrm{Ai}(\xi)J_{m'}((k_b^2-q^2)^{1/2}\rho), \quad (4)$$

where the argument of the regular Airy function Ai is

$$\xi(z,q) = -(2F)^{1/3}\left(z+\frac{q^2}{2F}\right) \quad (5)$$

and where $J_{m'}$ is a Bessel function. Assuming that in region II of the frame-transformation treatment the static electric field can be neglected, we expand $\psi^{(0)}_{bm'E}$ as

$$\psi^{(0)}_{bm'E}(q,\mathbf{r}) = \sum_{l'} s_{l'm'}(k_b,q)j_{l'}(k_b r)Y_{l'm'}(\hat{r}), \quad (6)$$

where $j_{l'}$ is the spherical Bessel function and $s_{l'm'}(k_b,q)$ are the expansion coefficients of the electric-field-dependent wave function in field-free wave functions. The method for obtaining the frame-transformation coefficients $s_{l'm'}$ and their explicit expression is given in Appendix A.

The Green's function can be written as

$$G^- = G^-_0 + \Delta G^-, \quad (7)$$

where G^-_0 is the Green's function in the absence of the field (i.e., the free-particle Green's function) and ΔG^- is the correction due to the field. As shown in Appendix B, a convenient separable expression for ΔG^- can be used to solve the Lippman-Schwinger equation, Eq. (3), analytically. However, our calculations have shown that this correction has almost no influence on the results for the cross sections. Therefore for simplicity in what follows we make the approximation $G^- = G^-_0$, which in any case is appropriate in region II. The more rigorous treatment including ΔG^- is given in Appendix B.

2. *Frame transformation*

Equation (6) gives the frame transformation for an electron moving only in the external electric field. We need, however, a frame transformation for the solutions of Eq. (3), which include all of the many-body electron-atom interactions. It is straightforward to show that to a good approximation the frame transformation required is the same as in Eq. (6).

Let us introduce a set of functions satisfying the following system of integral equations for a detached electron scattering from the atomic residue,

$$\zeta^-_{a[b']E}(\mathbf{r}) = j_{l'}(k_b r)Y_{l'm'}\delta_{ab} - \sum_c \int (G^-_0)_{aE}(\mathbf{r},\mathbf{r}')U_{ac}(\mathbf{r}')\zeta^-_{c[b']E}(\mathbf{r}')d\mathbf{r}', \quad (8)$$

where $[b']$ stands for the set of quantum numbers $bl'm'$ characterizing an asymptotic state of the atom-electron system. If we now express the solution for $\psi^-_{abEm'}$ in Eq. (3) in the form

$$\psi^-_{abm'E}(q,\mathbf{r}) = \sum_{l'} s_{l'm'}(k_b,q)\zeta^-_{a[b']E}(\mathbf{r}), \quad (9)$$

we see that Eq. (3) is satisfied provided G^- is replaced by G^-_0, the Green's function in the absence of the external electric field. As long as we are in region II this is a valid approximation. Hence the frame-transformation coefficients $s_{l'm'}(k_b,q)$ in Eq. (9) are the same as in Eq. (6). Their derivation is given in Appendix A.

The functions $\zeta^-_{a[b']E}(\mathbf{r})$ are the solutions of the many-body problem in region I. In this work , these functions are actually computed by solving the adiabatic hyperspherical equations (cf. Ref. [18]) and transforming the solutions to the independent electron states indicated by the asymptotic quantum numbers $[b']E$. The precise relation between the solutions of the Lippman-Schwinger Eq. (8) and the adiabatic hyperspherical functions of Ref. [18] will be specified below when we present our cross-section formulas.

Consider here, however, another frame transformation which should be carried out in region II. The quantum numbers b characterizing the atomic states are given in the absence of the external field as $b \equiv nlm$. However, this basis should be modified for $F \neq 0$ due to the linear Stark effect in hydrogen. Since the electric-field strengths considered in the present calculation are not so large as to affect the atomic states strongly, we may use a perturbative treatment. Consider specifically the n=2 states in H. We define the following four Stark substates in terms of the unperturbed functions:

$$\Phi^{\pm}_0 = \frac{1}{\sqrt{2}}(\Phi_{2s0} \pm \Phi_{2p0}), \quad (10)$$

$$\Phi_{\pm 1} = \Phi_{2p\pm 1}. \quad (11)$$

Thus in the presence of the external field, the two states $b \equiv nlm$ are mixed for m=0 to become the two Stark levels $2s \pm 2p$. Also, the thresholds for the excitation of the different Stark substates are shifted in accordance with the Stark-shift formula. This treatment of the Stark effect for atomic states is similar to the perturbative inclusion of the spin-orbit interaction in scattering theory [25]. For these reasons for H($n = 2$) we introduce the Stark state quantum number λ to replace l (i.e., $\lambda = +$ or $-$ for m=0 and $\lambda = +1$ for $m = \pm 1$) and introduce the unitary transformation matrix $U_{\beta b}$ defined in Eqs. (10) and (11) to transform from the representation $b \equiv nlm$ to $\beta \equiv n\lambda m$.

3. *Cross-section formulas*

We introduce now the photodetachment transition amplitude in the absence of the electric field:

$$X_{bl'm'E} \equiv X_{[b']E} = \left\langle \mathcal{A}\sum_a \Phi_a(\mathbf{r}_A)\zeta^-_{a[b']E}(\mathbf{r})|D|\Psi_i(\mathbf{r}_A,\mathbf{r})\right\rangle, \quad (12)$$

where D is the dipole operator for a one-photon transition and $b \equiv nlm$. This transition amplitude is for a detachment transition to a final state having total energy E in which the H atom is left in the nlm state and the photodetached electron is in the $l'm'$ state. It is directly related to the amplitudes $X^{(1)1M}_{nl,kl'}$ for the corresponding transition introduced in Eqs. (18) and (19) of Ref. [18]:

$$X_{bl'm'E} = \left(\frac{\pi}{2k}\right)^{1/2} i^{l'} \langle lml'm' \mid 1M\rangle X^{(1)1M}_{nl,kl'}. \quad (13)$$

In Eq. (13), the amplitudes $X^{(n_p)LM}_{nl,kl'}$ introduced in Ref. [18] have superscripts indicating that in a one-photon (i.e., n_p=1) transition from the $^1S^e$ H^- ground state the total angular momentum of the H(n = 2)-e^- system is L=1; M is the component along the z-axis and is determined by the polarization of the photon: $M = \pm 1$ for right (+) or left (−) circularly polarized light propagating along the electric field, and $M = 0$ for linearly polarized light with the direction of polarization parallel to the electric field. More general cases can be treated easily and an example of linear perpendicular polarization is given in Sec. IV. The Clebsch-Gordan coefficient projects the $L = 1, M$ state onto the independent electron state $lml'm'$, and the factor $i^{l'}(\pi/2k)^{1/2}$ gives the proper energy normalization for the wave function. (In order to obtain this factor one notes that the final-state wave functions in Ref. [18] are momentum normalized. Comparing their asymptotic behavior with the asymptotic behavior of the functions $\zeta_{a[b']E}(\mathbf{r})$ [cf. Eq.(8)] gives the desired factor.) Thus, to reiterate, we have carried out our analytic work using Eq. (12) for the transition amplitudes in region I; these amplitudes are actually calculated, however, using Eq. (13) and the amplitudes $X^{(1)1M}_{nl,kl'}$ calculated in the adiabatic hyperspherical approximation in Ref. [18].

The transition amplitudes in the presence of the external electric field are calculated by making the two-frame transformations discussed in Sec. II B 2 above, i.e.,

$$Z_{\beta m'E}(q) = \sum_{l'} s_{l'm'}(k_\beta, q) X_{\beta l'm'E}, \quad (14)$$

where

$$X_{\beta l'm'E} \equiv \sum_b U_{\beta b} X_{bl'm'E}. \quad (15)$$

Notice that the detached-electron energy $k_\beta^2/2$ depends on the Stark state β of the atom. The cross section for photodetachment in an external electric field can now be represented as [12]

$$\sigma_\beta = \frac{4\pi^2\omega}{c} \sum_{m'} \int_{-\infty}^{k_\beta^2/2} \mid Z_{\beta m'E}(q) \mid^2 d\left(\frac{q^2}{2}\right), \quad (16)$$

where ω and c are the frequency and velocity of the incident light, $k_\beta^2/2$ is the total electron energy in the final state, and $q^2/2$ is the energy of the electron motion along the electric field. Substituting now Eq. (14) into Eq. (16), we obtain for the cross section

$$\sigma_\beta = \frac{4\pi^2\omega}{c} \sum_{l'l''m'} X_{\beta l'm'E} X^*_{\beta l''m'E} \mu^{m'}_{l'l''}(k_\beta), \quad (17)$$

$$\mu^{m'}_{l'l''}(k_\beta) = \int_{-\infty}^{k_\beta^2/2} s_{l'm'}(k_\beta, q) s^*_{l''m'}(k_\beta, q) d\left(\frac{q^2}{2}\right). \quad (18)$$

Explicit expressions for the coefficients $\mu^{m'}_{l'l''}$, which contain the entire effect of the electric field, are given in Appendix C. We note here the limiting value of the coefficients [26]:

$$\lim_{F\to 0} \mu^{m'}_{l'l''}(k) = \delta_{l'l''} \frac{2k}{\pi}. \quad (19)$$

When Eqs. (13) and (19) are substituted into Eq. (17), we recover, as expected, the zero-field cross-section formula given in Eq. (33) of Ref. [18]. Note also that if the z component of the total angular momentum M has a definite value, then the sum over m' in Eqs. (16) and (17) contains only one term given by

$$m' = M - m_\beta, \quad (20)$$

where m_β is the (specified) z component of the final-state atomic angular momentum and M is defined by the polarization of the incident photon, as discussed above.

4. Near-threshold effects of long-range dipole fields

One modification of the cross-section formulas presented in Eqs. (16) and (17) should be done due to the long-range nature of the final-state interaction. The degeneracy of the $2s$ and $2p$ levels for F=0 produces the long-range dipole interaction between the electron and the atomic residue [27]. This interaction controls the threshold behavior of the cross sections and leads to spurious features if included in the frame-transformation theory in the region of space where the electric-field effects dominate. To see this clearly let us note that in the absence of the long-range interaction the matrix element $X_{\beta l'm'E}$ behaves as $k_\beta^{l'}$. From Eqs. (17) and (19) we see that at $F = 0$ the cross section behaves according to the Wigner law $\sigma_\beta \propto k_\beta^{2l'+1}$ and at $F \neq 0$ it is finite at the zero-field threshold since the electric field removes the threshold. However, after the inclusion of the long-range dipole interaction the threshold laws change. The matrix element $X_{\beta l'm'E}$ starts to behave like $k_\beta^{-1/2}$ and oscillates near threshold [18,27]. This behavior leads to the divergence of σ_β as k_β^{-1} when $F \neq 0$. In order to eliminate this spurious behavior, we have to cut off the long-range dipole interaction at distances dominated by the electric-field interaction. It is more convenient to formulate the cutoff procedure in energy space. Let us choose some boundary value E_c of the electron energy below which the behavior of the zero-field matrix elements is controlled by the long-range dipole interaction. A reasonable choice for this energy in our case is the position of the $^1P^o$ shape resonance, which in our calculations lies at 41 meV above the zero-field thresh-

old. For $E > E_c$ we use the matrix elements calculated with inclusion of the long-range dipole interaction, and for $E < E_c$ we multiply all matrix elements by a factor which gives the Wigner behavior at the threshold and at the same time gives a smooth transition to the region $E > E_c$. This procedure gives a reasonable extrapolation with the proper threshold behavior for $F \neq 0$. However, for high enough fields this approach as well as the whole approach of frame-transformation theory fails since the atomic-field region and the electric-field region start to overlap strongly. As follows from Lin's calculations [10], this effect occurs at fields above F=1 MV/cm. Therefore higher fields have not been considered in the present calculations.

III. CALCULATIONS FOR ZERO FIELD

Our results for the total photodetachment cross section in the absence of an electric field are discussed in detail in Ref. [18]. The cross section above the $n = 2$ threshold of H is about a factor of 1.75 wider in energy than is measured experimentally [5]. Detailed comparisons of experiment with theory have recently been presented by Halka *et al.* [28]. The peak value of our cross section is about a factor of 2.5 lower than that given by the 160-configuration J-matrix calculations of Broad and Reinhardt [29]. Nevertheless, the cross section is in much better agreement with the relative experimental measurements than is the one obtained by a simple close-coupling calculation [30]. Also, as we shall see in Sec. IV, the corresponding matrix elements can be used to make certain conclusions about the behavior of the cross sections for nonzero fields.

IV. RESULTS AND DISCUSSION

Calculations have been performed for two types of polarization: linear and parallel to the external electric field (π polarization) and circular with the direction of photon propagation along the electric field ($\sigma^{\pm}$ polarization). The experimental data [5–7] on photodetachment in an external field were obtained with a polarization state which "favors π," although its exact preparation was affected both by a finite angle between the negative-ion beam and the laser beam and by optical activity within the prisms used in the experiment.

Some data [6,7] were also obtained for light linearly polarized perpendicular to the external field. Comparison of theory with this set of experimental data requires some care. Let us consider the relation between the dipole op-

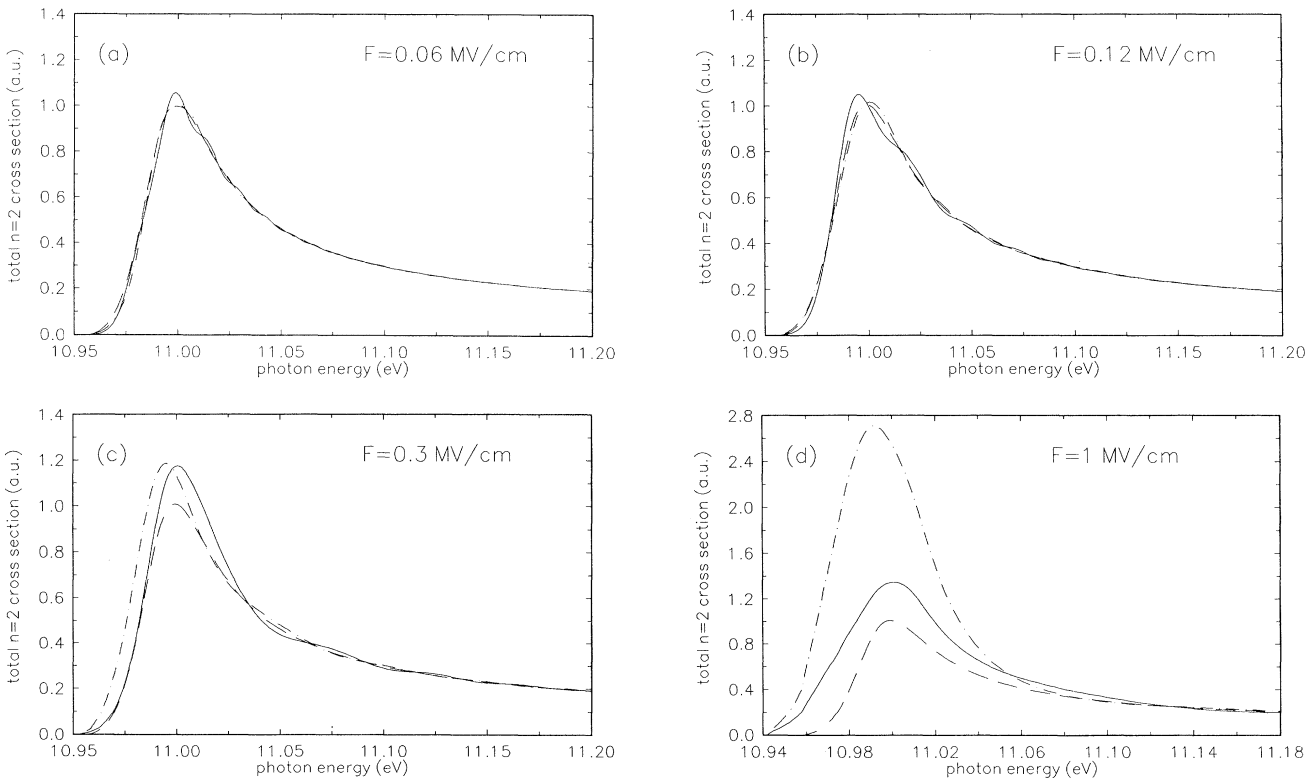

FIG. 1. Total cross section for photodetachment of H^- with excitation of the n=2 states in an external electric field of strength F. Dot-dashed curve: linear polarization parallel to the static field (π polarization); solid curve: circular polarization with the direction of light propagation parallel to the static field (σ^+ polarization); dashed curve: photodetachment in zero field, which is independent of the light polarization. (a) F=0.06 MV/cm, (b) F=0.12 MV/cm, (c) F=0.3 MV/cm, (d) F=1 MV/cm.

erator D^x corresponding to the polarization along the x axis, and the operators $D^{\pm}$ corresponding to right and left circular polarization:

$$D^x = \frac{1}{\sqrt{2}}(D^+ + D^-). \tag{21}$$

We obtain two terms in Eq. (13) containing $\delta_{m',\pm 1-m}$, and the final expression for the cross section is

$$\sigma_m^{\perp} = \frac{1}{2}(\sigma_m^+ + \sigma_m^-) \tag{22}$$

or, using the symmetry of the problem with respect to the transformation $M \to -M$, $m \to -m$,

$$\sigma_m^{\perp} = \frac{1}{2}(\sigma_m^+ + \sigma_{-m}^+). \tag{23}$$

In Fig. 1 we present the total cross section [i.e., summed over all final atomic states β; cf. Eqs. (16) and (17)] as a function of energy for four values of the electric-field strength F. The electric-field effect is clearly present for both types of polarization for photon energies below 11.07 eV. The ripple structure of the cross section (which appears due to interference effects [2]) is noticeable for circularly polarized light. [Note that according to Eq. (23) the same result holds in the case of linear perpendicular polarization for the cross section summed over all final Stark substates. Unfortunately, the experimental data for the case of linear perpendicular polarization (which is called σ polarization in Ref. [7]) have error bars which are too large to make definite conclusions about the existence of the ripple structure.] For larger values of F the ripples have a smaller frequency. This can be understood by examining the quasiclassical expression [2] for the modulation factor $\cos(2k_\beta^3/3F + \delta)$, where δ is a constant phase. For F=1 MV/cm [cf. Fig. 1(d)], the electric field is too large for the cross section to exhibit ripple structure near threshold. However, the electric field does affect very strongly the magnitude of the cross section, especially for π polarization.

In order to understand the origin of the ripple structure, it is instructive to analyze the partial cross sections for excitation of different Stark substates. These are presented in Figs. 2 and 3 for four values of the electric field. We find that the ripple-type structure appears only in those partial cross sections for which the magnetic quantum number of the detached electron is $m' = 0$. In this case the electron moves classically along the electric field and thus conditions for interference between the direct and the reflected paths for electron es-

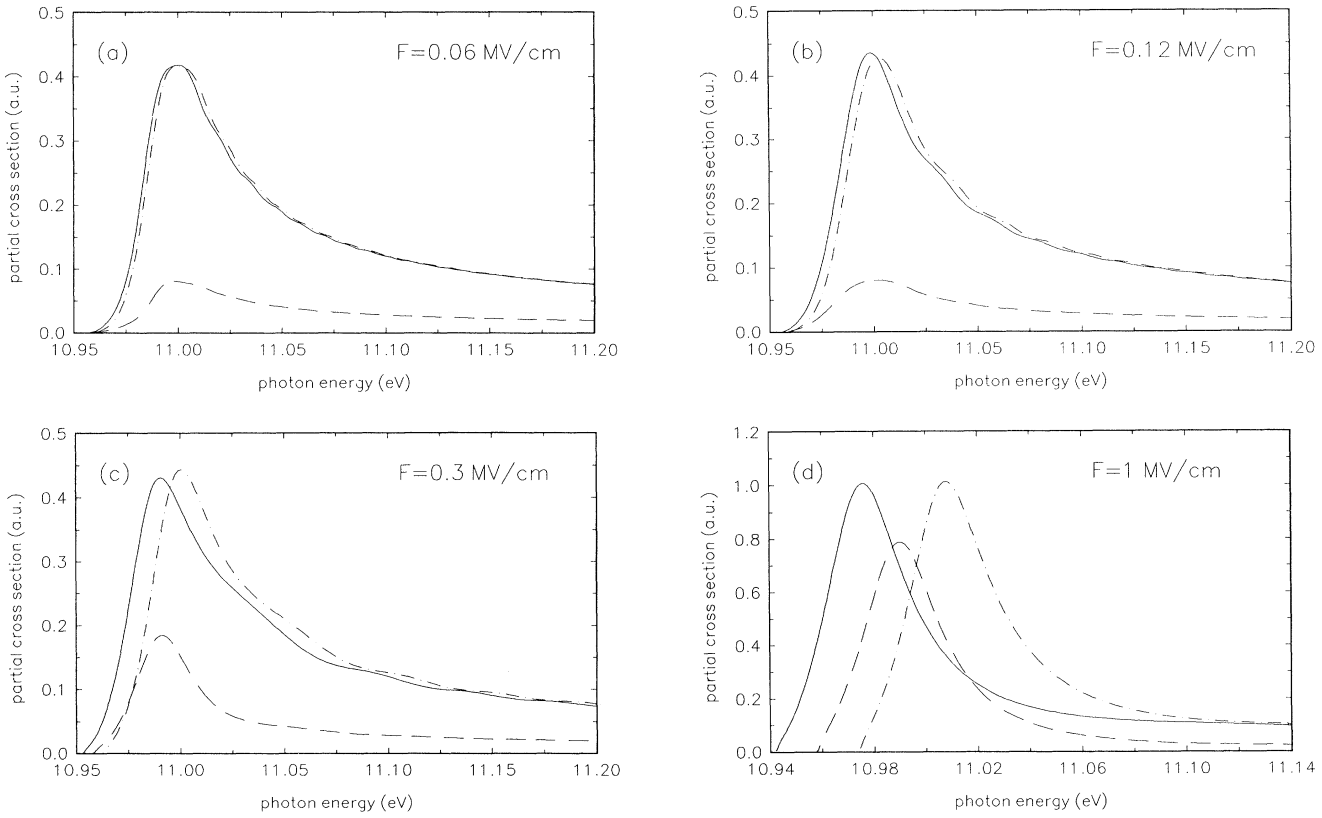

FIG. 2. Cross sections for photodetachment of H^- in a static electric field F by π-polarized light with excitation of the Stark substates: $\gamma_L + H^- \to H(n = 2, \lambda, m) + e^-(m')$. Solid curve: $\lambda = +$, m=0, m'=0 [in the notation presented in the text below Eq. (11)]; dashed curve: λ=1, $m = \pm 1$, $m' = \mp 1$ (these cross sections are equal); dot-dashed curve: $\lambda = -$, $m = 0$, $m' = 0$. (a) F=0.06 MV/cm, (b) F=0.12 MV/cm, (c) F=0.3 MV/cm, (d) F=1 MV/cm.

cape along the electric field are most favorable [2]. The interference structure is especially well pronounced in the cross section for excitation of the $m = 1$ atomic substate with σ^+-polarized photons [cf. Figs. 3(a)–3(c)]. It occurs even at the relatively low field F=60 kV/cm. The interference structure in the cross section for excitation of the $m = 0$ substates by π-polarized photons [cf. Figs. 2(a)–2(c)] is not as well pronounced.

Figures 2 and 3 for the partial photodetachment cross sections clearly indicate that the quantum-mechanical interference stemming from the two paths for electron escape is most noticeable when the photoelectron has m'=0. This begs the question why the total cross sections shown in Figs. 1(a)–1(c) only exhibit ripple structure for the case of σ-polarized light even though the case of π-polarized light has two channels ($\lambda = +$ or $-$) having m'=0. From Figs. 2(a)–2(c) we surmise that the ripple structures in these two partial cross sections are "out of phase" as a function of photon energy. Thus when the partial cross sections in Fig. 2 for π polarization are added, the total does not have noticeable ripple structure.

Another important result of our calculation is the finding that the rescattering effect is weak. This effect, which is represented by the second term in Eq. (B17), is due to the scattering of the reflected electron amplitude by the atom, and was discussed in Ref. [14] for photodetachment of H^- with formation of H in the ground state. There the effect turned out to be very weak due to the small strength of the interaction between the detached electron and the hydrogen atom in its ground state. The interaction of the detached electron with the excited hydrogen atom was expected in the present calculations to be much stronger due to the long-range dipole interaction. However, the present calculations (carried out according to the equations presented in Appendix B) show that even in this case the rescattering effect is weak, due to the resonance behavior of the cross section near threshold. The influence of the rescattering effect on the cross section is nearly unnoticeable on the scale of our figures and never exceeds 2.5%. We therefore do not present these cross sections in the figures.

In order to analyze the enhancement of the peak value of the cross section as a function of the electric field, we have investigated how the strength of the resonance, a quantity introduced by Bryant *et al.* [5], depends on the electric field. The strength of a resonance is defined as [5]

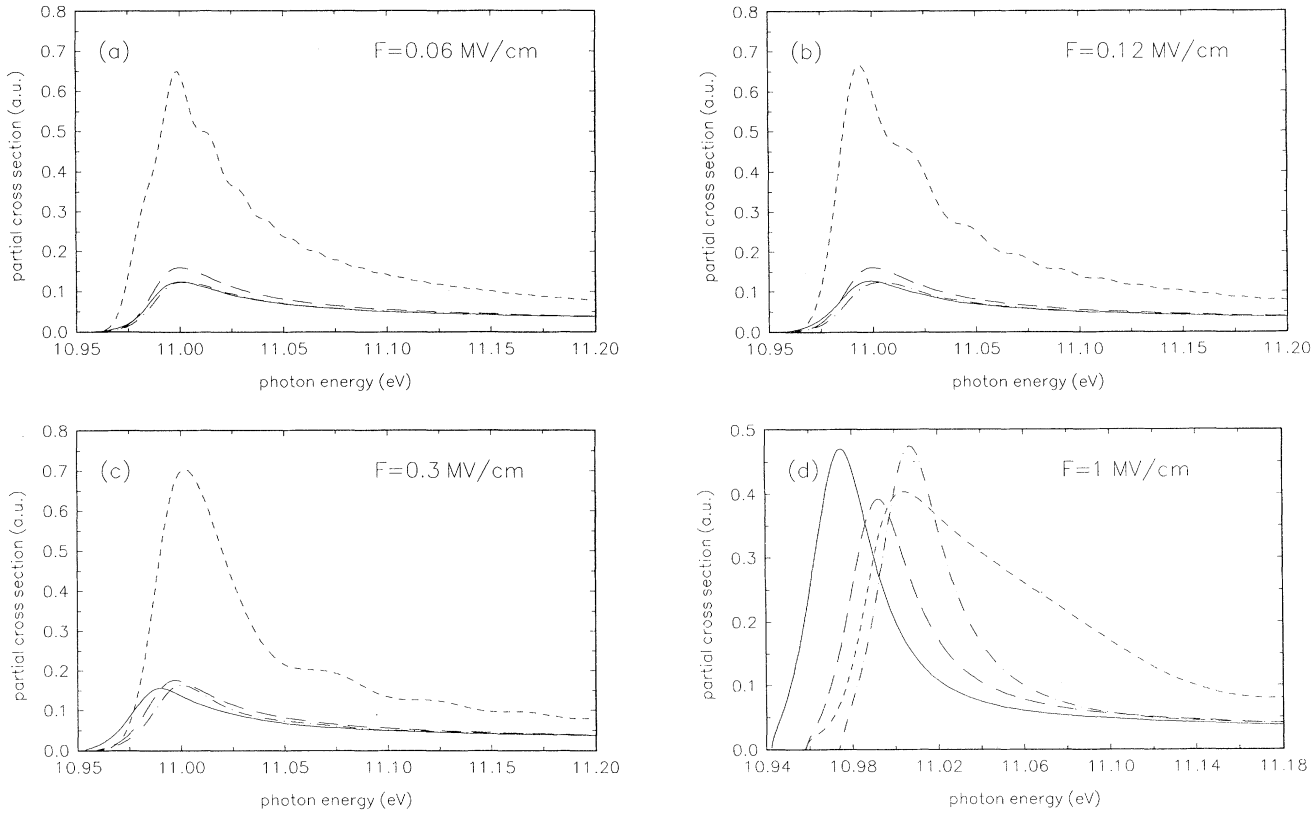

FIG. 3. Cross sections for photodetachment of H^- in a static electric field F by σ^+-polarized light with excitation of the Stark substates: γ_C+$H^- \rightarrow H(n = 2, \lambda, m)$+$e^-(m')$. Solid curve: $\lambda = +$, $m = 0$, $m' = +1$ [in the notation presented in the text below Eq. (11)]; long-dashed curve: $\lambda = 1$, $m = -1$, $m' = 2$; short-dashed curve: $\lambda = 1$, $m = +1$, $m' = 0$; dot-dashed curve: $\lambda = -$, $m = 0$, $m' = +1$. (a) F=0.06 MV/cm, (b) F=0.12 MV/cm, (c) F=0.3 MV/cm, (d) F=1 MV/cm.

$$Q_{\rm res} = \int dE \frac{\sigma(E) - \sigma_a - \sigma_b}{\sigma_a + \sigma_b}, \tag{24}$$

where $\sigma(E)$ is the total detachment cross section and σ_a and σ_b are obtained by fitting the shape resonance to the Fano profile formula [31]

$$\sigma_{\rm Fano}(E) = \sigma_a \frac{(q+\epsilon)^2}{1+\epsilon^2} + \sigma_b, \tag{25}$$

where

$$\varepsilon = 2(E - E_0)/\Gamma. \tag{26}$$

In Eqs. (25) and (26), ε is a reduced energy defined by Eq. (26) in terms of the resonance position E_0 and resonance width Γ, σ_a is the part of the cross section which interacts with the resonance, and σ_b is the background cross section. Fitting Eqs. (25) and (26) to experimental data provides values for the parameters σ_a, σ_b, E_0, and Γ.

Substituting now Eqs. (25) and (26) into Eq. (24), one obtains the following result for the resonance strength [5]:

$$Q_{\rm res} = \frac{\pi\sigma_a(q^2-1)\Gamma}{2(\sigma_a + \sigma_b)}. \tag{27}$$

The results of our fitting procedure for the Fano parameters (to our theoretically calculated curves) were subject to considerable irregular variations with the electric-field strength F. Interestingly enough, the same kind of variation, but to a much greater extent, occurred in the fits to the experimental data [5–7] (see, e.g., Fig. 20 in Ref. [5], which shows the dependence of the shape parameter q on F). Whereas variations of the experimentally fitted values might have occurred due to experimental uncertainties, there are two physical reasons for these variations: namely, low fields the shape of the curve is affected by the ripple structure and the Fano formula [cf. Eq. (25)] cannot fit this oscillatory structure. At higher fields the Stark splitting of the atomic states becomes important, and the total cross section, which is the sum of the partial cross sections for excitation of different Stark substates with different thresholds, again cannot be represented by the Fano profile. For a more complete analysis, parametrization of the partial cross sections would be necessary, as is done for the case F=0 in Ref. [28], using an appropriate generalization of the Fano profile formula [32].

However, for the purpose of comparison with the experiment [6], we present in Fig. 4 a piecewise-spline fit to our data for the strength of the shape resonance. The results confirm the experimentally observed growth of the resonance strength $Q_{\rm res}$ with the electric field, although the absolute magnitude of the theoretical values is about a factor of 2 smaller than that of the experimental values. A strong dispersion of the experimental data does not allow one to make more definite conclusions.

In Fig. 5 we present the fitted resonance width Γ as a function of the electric-field strength F. At lower fields, Γ cannot be determined uniquely due to the ripple-structure effect mentioned above; therefore we present

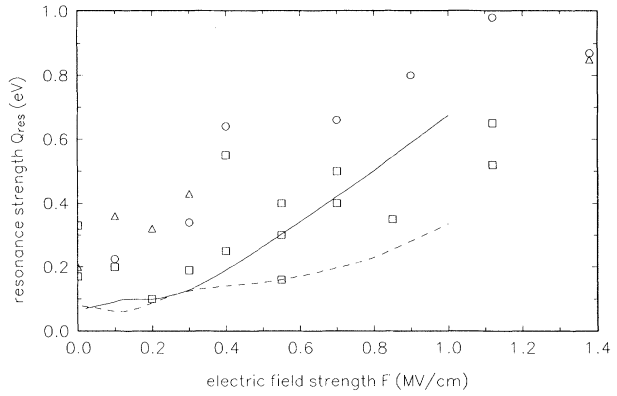

FIG. 4. The resonance strength $Q_{\rm res}$ as a function of the electric field [cf. Eq. (27)]. Theory: solid curve, π polarization; dashed curve, σ polarization. Experiment [6]: triangles, π polarization; circles, σ polarization; squares, unpolarized data.

theoretical values only for $F \geq 0.4$ MV/cm. Experimental data presented in Refs. [5,6] are also very dispersed. Figure 5 shows two possible analytical fits [5] to the experimental data for the case of π polarization. Comtet *et al.* [7] detected a slight decrease (of about 3.3±0.9%) of the width when increasing the field from 0 to 0.24 MV/cm. However, this decrease lies well within the uncertainty caused by the ripple structure.

For $F = 0$ our result for the width is too high (about a factor of 1.75), as discussed above. Our results for higher fields are much closer to the experimental results. For fields above 1 MV/cm, when the atomic-field potential and the electric-field potential overlap substantially, our results begin to become unreliable since, as we indicated above, the frame-transformation treatment fails in this case.

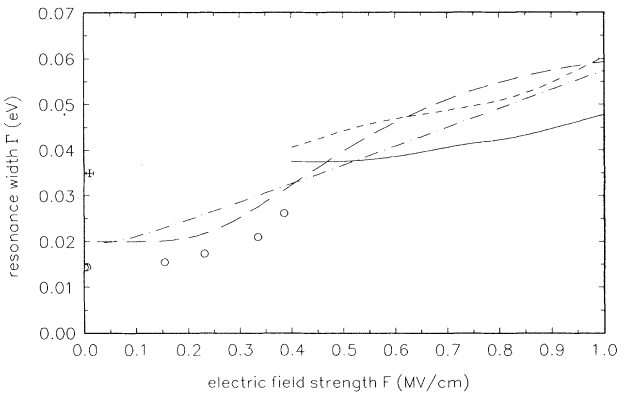

FIG. 5. The width Γ of the shape resonance as a function of the electric-field strength F. Solid curve: present calculations, π polarization; short-dashed curve: present calculations, σ polarization. The cross gives our value at F=0. Long-dashed and dot-dashed curves: two analytical fits to the experimental data [5]; circles: theoretical calculations of Wendoloski and Reinhardt [9].

Our results confirm the theoretical findings of Lin [10], who found very high stability for the shape resonance up to fields of 1 MV/cm. Wendoloski and Reinhardt's results [9], obtained via the method of complex coordinate rotation, exhibit a monotonic increase of the width at low fields. Their data represent the imaginary part of the S-matrix pole in the complex energy plane and may not reflect the ripple structure of the photodetachment cross section. (However their results are most likely more precise for the magnitude of the width.)

V. CONCLUSIONS

Using photodetachment matrix elements calculated in the adiabatic hyperspherical approximation at F=0 one can make certain conclusions about photodetachment of H^- with excitation of H(n=2) in the presence of an external electric field. We find that the electric-field-induced ripple structure in the total cross sections is not noticeable for π polarization, but is relatively well pronounced for σ polarization. However, noticeable ripple structures are obtained for both polarizations in the case of partial cross sections corresponding to a zero value for the magnetic quantum number of the detached electron. The case of excitation of the m=1 atomic Stark substate by circularly polarized photons is especially favorable in this respect. On the other hand, the rescattering effect resulting from interaction of the detached electron with the H(n=2) excited states is found in all cases to have no significant effect on the cross sections.

Our results confirm a strong enhancement of the strength of the shape resonance observed experimentally by Butterfield *et al.* [6]. Accurate values of the resonance width cannot be obtained for small values of the electric-field strength F because of the ripple structure in the cross section. However, the overall behavior of the width as a function of the electric-field strength for higher values of F confirms the earlier theoretical prediction [10] as well as experimental observations [5,7] of a high stability of the shape resonance with increasing field strength F.

ACKNOWLEDGMENTS

The authors are grateful to Dr. V. Z. Slonim for many helpful discussions, particularly regarding calculations of integrals containing Airy functions, and to Dr. H. C. Bryant for useful comments on experimental data. The work of I.I.F. has been supported in part by the National Science Foundation through Grant No. PHY92-07986. The work of N.Y.D. and A.F.S. has been supported in part by the U.S. Department of Energy, Office of Basic Energy Sciences, Division of Chemical Sciences, under Grant No. DE-FG02-88ER13955.

APPENDIX A: EXPRESSIONS FOR FRAME-TRANSFORMATION COEFFICIENTS

In order to obtain the frame-transformation coefficients $s_{lm}(q)$ we follow the procedure developed in Refs. [11,14]. Consider the function in Eq. (4). At small distances

$$\frac{2^{1/3}}{F^{1/6}}\mathrm{Ai}(\xi) = \nu(q)\sin(qz) + \tau(q)\cos(qz), \tag{A1}$$

where

$$\nu(q) = -\frac{2^{2/3}F^{1/6}}{q}\mathrm{Ai}'(\xi(0,q)), \tag{A2}$$

$$\tau(q) = \frac{2^{1/3}}{F^{1/6}}\mathrm{Ai}(\xi(0,q)), \tag{A3}$$

where $\xi(0,q) = -q^2/(2F)^{2/3}$ [cf. Eq. (5)] and the prime indicates the derivative. The function $\psi^{(0)}$ can be expanded in spherical harmonics:

$$[\nu(q)\sin qz + \tau(q)\cos qz]J_m((k^2-q^2)^{1/2}\rho)\frac{e^{im\phi}}{(2\pi)^{1/2}} = \sum_l s_{lm}(k,q)j_l(kr)Y_{lm}(\theta,\phi). \tag{A4}$$

The simplest way to obtain explicit expressions for the coefficients $s_{lm}(q)$ is to consider the limit of Eq. (A4) as $r \to 0$. The final expressions are

$$s_{00}(k,q) = \tau(q)\sqrt{2}, \tag{A5}$$

$$s_{10}(k,q) = \frac{3q\nu(q)}{k}\sqrt{\frac{2}{3}}, \tag{A6}$$

$$s_{11}(k,q) = \frac{\tau(q)}{k}\sqrt{3(k^2-q^2)}, \tag{A7}$$

$$s_{21}(k,q) = \frac{\nu(q)q}{k^2}\sqrt{15(k^2-q^2)}, \tag{A8}$$

$$s_{20}(k,q) = \sqrt{\frac{5}{2}}\tau(q)\left(1-\frac{3q^2}{k^2}\right), \tag{A9}$$

$$s_{22}(k,q) = \frac{\sqrt{15}}{2}\tau(q)\left(1-\frac{q^2}{k^2}\right). \tag{A10}$$

This set of coefficients allows one to perform calculations in which the maximum possible value of the electron angular momentum is equal to 2. The coefficients s_{10} and s_{11} were previously obtained by Rau and Wong [11].

APPENDIX B: FRAME-TRANSFORMATION EXPRESSION FOR THE GREEN'S FUNCTION AND INCLUSION OF THE RESCATTERING EFFECT

If the energy of the outgoing electron is above the threshold, the Green's function (7) may be written in the form [16]

$$G^+ = G_0^+ + ye^{ik(z+z')}, \tag{B1}$$

where for high enough k [16]

$$y = \frac{F}{4\pi ik^2}e^{2ik^3/3F}. \tag{B2}$$

The function G^- can be obtained from Eq. (B1) by complex conjugation.

Equation (B2) diverges at the threshold when $k \to 0$ and should be modified in that energy region. Let us rewrite Eq. (B1) for $\mathbf{r}' = 0$:

$$G^+(\mathbf{r},0) = \frac{e^{ikr}}{2\pi r} + ye^{ikz}. \tag{B3}$$

Equation (B3) may be solved for y to give

$$y = \lim_{r\to 0}\left[G^+(\mathbf{r},0) - \frac{1}{2\pi r} - \frac{ik}{2\pi}\right]. \tag{B4}$$

To calculate the right-hand side of Eq. (B4), we employ the integral representation for the Green's function [33]:

$$2\pi G^+(\mathbf{r},0) = \int_{-\infty}^{k^2/2} d\left(\frac{q^2}{2}\right) J_0\big((k^2-q^2)^{1/2}\rho\big) g(q^2,z), \tag{B5}$$

where

$$g(q^2,z) = \frac{2\pi}{(2F)^{1/3}}\mathrm{Ai}(\xi_>)\mathrm{Ci}(\xi_<), \tag{B6}$$

$$\xi_> = \max[\xi(z,q),\xi(0,q)], \qquad \xi_< = \min[\xi(z,q),\xi(0,q)], \tag{B7}$$

and $\mathrm{Ci}(\xi)$ is the irregular Airy function which satisfies the asymptotic boundary condition of the outgoing wave. Following Demkov and Drukarev [33], we introduce the representation

$$\frac{1}{r} = i\int_{i\infty}^{k} e^{iqr}dq - ik + O(r) \tag{B8}$$

and approach the limit in Eq. (B4) along the z-axis. Substituting Eq. (B8) to the right-hand side of Eq. (B4) gives

$$2\pi y = \lim_{p\to\infty}\lim_{z\to+0}\left[\int_{ip}^{k} qg(q^2,z)dq - i\int_{ip}^{k} e^{iqz}dq\right]. \tag{B9}$$

Calculation of this limit using the asymptotic expressions for the Airy functions [34] leads to the result

$$y = \frac{(2F)^{1/3}}{2}[\mathrm{Ai}'(-\eta)\mathrm{Ci}'(-\eta) + \eta\mathrm{Ai}(-\eta)\mathrm{Ci}(-\eta)] - \frac{ik}{2\pi}, \tag{B10}$$

where $\eta = k^2/(2F)^{2/3}$. In Fig. 6 we compare the exact Green's function, given by Eq. (5) of Ref. [13], with the approximate representation given by Eqs. (B1) and (B10). We see that this representation gives a good extrapolation of the asymptotically exact formula down to the threshold.

Let us turn now to the solution of the basic Eq. (3). Since the electric-field correction to the Green's function is separable, we can again express the solution in terms of the functions $\zeta^-_{a[b']E}$, defined in Eq. (8). Equation (9) for the channel wave function becomes

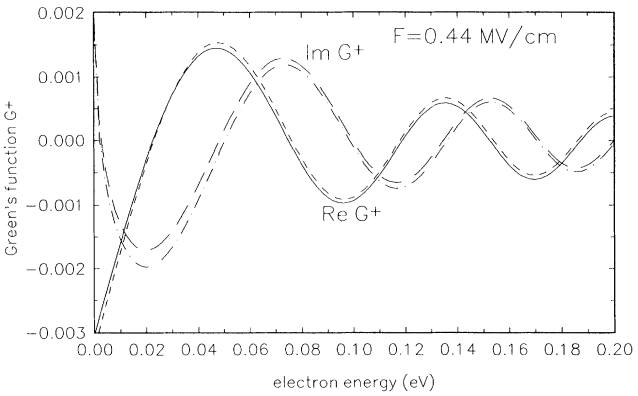

FIG. 6. Real and imaginary parts of the Green's function $G^+(\mathbf{r}_1,\mathbf{r}_2)$ for an electron in a static electric field F=0.44 MV/cm for $r_1 = 4$, $r_2 = 5$, $z_1 = 4$, $z_2 = -2.5$. The real part $\mathrm{Re}G^+$: solid curve, exact result using Eq. (5) of Ref. [13]; short-dashed curve, approximate result using Eqs. (B1) and (B10). The imaginary part $\mathrm{Im}G^+$: long-dashed curve, exact result; dash-dotted curve, approximate result.

$$\psi^-_{abm'_b}(q,\mathbf{r}) = \sum_{l'_b} s_{l'_b m'_b}(q)\zeta^-_{a[b']}(\mathbf{r}) - \sum_{c,l'_c}\zeta^-_{a[c']}(\mathbf{r})i^{-l'_c}[4\pi(2l'_c+1)]^{1/2}V_{cbm'_b}(q), \tag{B11}$$

where

$$V_{abm'_b}(q) = y^*\sum_c \int e^{-ikz'}U_{ac}(\mathbf{r}')\psi^-_{cbm'_b}(q,\mathbf{r}')d\mathbf{r}', \tag{B12}$$

where $[b']$ stands for b, l'_b, m'_b, $[c']$ stands for c, l'_c, m'_c, and the second sum in Eq. (B5) contains only $m'_c = 0$. For simplicity we omit here and below the total energy index E. The coefficients $V_{abm'_b}(q)$ satisfy a system of algebraic equations which can be obtained by substitution of Eq. (B11) into Eq. (B12). However, for the electric-field strengths considered in this paper, the first-order term in y is sufficient. Thus we approximate Eq. (B12) by the first term in Eq. (B11),

$$V_{abm'_b}(q) = y^*\sum_c\sum_{l'_b} s_{l'_b m'_b}(q)\int e^{-ikz'}U_{ac}(\mathbf{r}')\zeta^-_{c[b']}(\mathbf{r}')d\mathbf{r}'. \tag{B13}$$

Using then the integral representation for the T matrix for electron scattering by the hydrogen atom,

$$T_{[a'][b']} = 4i(k_a k_b)^{1/2}\sum_c \int Y^*_{l'_a m'_a}(\hat{r}')j_{l'_a}(k_a r')U_{ac}(\mathbf{r}') \times\zeta^+_{c[b']}(\mathbf{r}')d\mathbf{r}', \tag{B14}$$

and the connection between the incoming and outgoing solutions $\zeta^-_{l_a m_a l_b m_b l'_b m'_b} = (\zeta^+_{l_a -m_a l_b -m_b l'_b -m'_b})^*$, we ob-

tain finally

$$V_{abm'_b}(q) = \frac{iy^*}{4(k_a k_b)^{1/2}} \sum_{l'_b l'_a} s_{l'_b m'_b}(q) i^{-l'_a} \times [4\pi(2l'_a+1)]^{1/2} T^*_{[a'][b']}, \tag{B15}$$

where the T-matrix element is evaluated for $m'_a = 0$. The latter condition results from the fact that the plane wave contributing to the Green's function (B1) propagates parallel to the electric field.

Equation (14) for the photodetachment matrix element in the presence of a static electric field can be generalized now as

$$Z_{bm'_b}(q) = \sum_{l'_b} s_{l'_b m'_b}(q) Q_{[b']}, \tag{B16}$$

where

$$Q_{[b']} = X_{[b']} + \pi i y \sum_{c,l'_c,l''_c} i^{l'_c + l''_c} (k_b k_c)^{-1/2} \times [(2l'_c+1)(2l''_c+1)]^{1/2} \times T_{[c'']}[b'] X_{[c']}. \tag{B17}$$

The cross section then takes the form

$$\sigma_b = \frac{4\pi^2 \omega}{c} \sum_{l'_b, l''_b} Q_{[b']} Q^*_{[b'']} \mu^{m'_b}_{l'_b l''_b}. \tag{B18}$$

The equations obtained above have a simple physical meaning. The first term in Eq. (B17) describes photodetachment without the external field and the second term describes photodetachment with formation of the hydrogen atom in the state c followed by rescattering of the photodetached electron leading to the state b.

In order to calculate the photodetachment amplitudes as given by Eq. (B17) we need the T-matrix elements for F=0. They were calculated in the present work using the adiabatic hyperspherical representation, as discussed in Ref. [18]. The long-range dipole interaction between the electron and the excited hydrogen atom is diagonal in the adiabatic hyperspherical representation, which makes the calculation of the scattering matrix easy. First, we calculate the adiabatic phase shifts and then convert them in the representation of the total angular momentum, as discussed by Liu and Starace [35]. The scattering matrix in the representation $| l_b m_b l' m' \rangle$ can then be obtained by standard angular momentum decoupling techniques. Since the external electric field intermixes the initial $L = 1$ state with the $L = 0$ and $L = 2$ states, calculations of the T matrix corresponding to these angular momenta as well as the one for $L = 1$ were performed.

APPENDIX C: INTEGRALS OF PRODUCTS OF THE FRAME-TRANSFORMATION COEFFICIENTS

In order to calculate the cross sections given by Eq. (17), we need to evaluate the integrals

$$\mu^{m'}_{l'l''}(k) = \int_{-\infty}^{k^2/2} s_{l'm'}(k,q) s_{l''m'}(k,q) d\left(\frac{q^2}{2}\right), \tag{C1}$$

where the explicit form of $s_{l'm'}(q)$ is given in Appendix A. Those expressions show that all integrals can be reduced to integrals of products of the Airy function Ai, its derivative, and powers of $\xi(0,q)$ [cf. Eq. (5)]. These integrals can be evaluated as suggested in Refs. [13,36]. Defining the parameter $\eta = k^2/(2F)^{2/3}$ and introducing the notation

$$(z^n f, g) \equiv \int_{-\infty}^{\eta} z^n f(-z) g(-z) dz, \tag{C2}$$

we obtain the following results for the integrals necessary for evaluating the coefficients $\mu^{m'}_{l'l''}(k)$ in Eq. (C1):

$$(\mathrm{Ai}, \mathrm{Ai}) = (\mathrm{Ai}')^2 + \eta \mathrm{Ai}^2, \tag{C3}$$

$$(\mathrm{Ai}', \mathrm{Ai}) = \tfrac{1}{2}\mathrm{Ai}^2, \tag{C4}$$

$$(z\mathrm{Ai}, \mathrm{Ai}) = \tfrac{1}{3}[\mathrm{Ai}'\mathrm{Ai} + \eta^2 \mathrm{Ai}^2 + \xi(\mathrm{Ai}')^2], \tag{C5}$$

$$(\mathrm{Ai}', \mathrm{Ai}') = -\tfrac{2}{3}\mathrm{Ai}\mathrm{Ai}' + \tfrac{1}{3}(\mathrm{Ai}, \mathrm{Ai}), \tag{C6}$$

$$(z\mathrm{Ai}', \mathrm{Ai}) = \tfrac{1}{2}(\mathrm{Ai}')^2, \tag{C7}$$

$$(z^2\mathrm{Ai}, \mathrm{Ai}) = \tfrac{1}{5}[(1+\eta^3)\mathrm{Ai}^2 + 2\eta \mathrm{Ai}\mathrm{Ai}' + \eta^2(\mathrm{Ai}')^2], \tag{C8}$$

$$(z\mathrm{Ai}', \mathrm{Ai}') = (z^2\mathrm{Ai}, \mathrm{Ai}) - \eta \mathrm{Ai}\mathrm{Ai}' - (\mathrm{Ai}', \mathrm{Ai}). \tag{C9}$$

In each of these equations the argument of the Airy function and its derivative on the right-hand sides equals $-\eta$. These equations allow the evaluation of $\mu^{m'}_{l'l''}$ for $l' \leq 2$.

[1] See, e.g., B. Gao and A.F. Starace, Phys. Rev. A **42**, 5580 (1990), and references therein.

[2] I.I. Fabrikant, Zh. Eksp. Teor. Fiz. **79**, 2070 (1980) [Sov. Phys. JETP **52**, 1045 (1980)].

[3] H.C. Bryant, A. Mohagheghi, J.E. Stewart, J.B. Donahue, C.R. Quick, R.A. Reeder, V. Yuan, C.R. Hummer, W.W. Smith, S. Cohen, W. Reinhardt, and L. Overman, Phys. Rev. Lett. **58**, 2412 (1987); J.E. Stewart, H.C. Bryant, P.G. Harris, A.H. Mohagheghi, J.B. Donahue, C.R. Quick, R.A. Reeder, V.Yuan, C.R. Hummer, W.W. Smith, and S. Cohen, Phys. Rev. A **38**, 5628 (1988).

[4] P.A.M. Gram, J.C. Pratt, M.A. Yates-Williams, H.C. Bryant, J.B. Donahue, H. Sharifian, and H. Tootoonchi, Phys. Rev. Lett. **40**, 107 (1978).

[5] H.C. Bryant, D.A. Clark, K.B. Butterfield, C.A. Frost, H. Sharifian, H. Tootoonchi, J.B. Donahue, P.A.M. Gram, M.E. Hamm, R.W. Hamm, J.C. Pratt, M.A. Yates, and W.W. Smith, Phys. Rev. **27**, 2889 (1983).

[6] K.B. Butterfield, C.J. Harvey, H.C. Bryant, D.A. Clark, J.B. Donahue, P.A.M. Gram, D. MacArthur, and W.W. Smith, in *Symposium on Atomic and Surface Physics, Contributions*, edited by F. Howorka, W. Lindinger, and T.D. Märk (STUDIA Studienförderungsgesellschaft m.b.H., Innsbruck, 1984), p. 50.

[7] G. Comtet, C.J. Harvey, J.E. Stewart, H.C. Bryant, K.B. Butterfield, D.A. Clark, J.B. Donahue, P.A.M. Gram,

D.W. MacArthur, V. Yuan, W.W. Smith, and S. Cohen, Phys. Rev. A **35**, 1547 (1987).
[8] J. Callaway and A.R.P. Rau, J. Phys. B **11**, L289 (1978).
[9] J.J. Wendoloski and W.P. Reinhardt, Phys. Rev. A **17**, 195 (1978).
[10] C.D. Lin, Phys. Rev. A **28**, 1876 (1983).
[11] A.R.P. Rau and H.-Y. Wong, Phys. Rev. A **37**, 632 (1988).
[12] M.L. Du and J.B. Delos, Phys. Rev. A **38**, 5609 (1988).
[13] V.Z. Slonim and F.I. Dalidchik, Zh. Eksp. Teor. Fiz. **71**, 2057 (1976) [Sov. Phys. JETP **44**, 1081 (1976)].
[14] I.I. Fabrikant, Phys. Rev. A **40**, 2373 (1989).
[15] V.Z. Slonim and C.H. Greene, Radiat. Eff. **122-123**, 679 (1991); and private communication.
[16] I.I. Fabrikant, Zh. Eksp. Teor. Fiz. **83**, 1675 (1982) [Sov. Phys. JETP **56**, 967 (1982)].
[17] J.H. Macek, J. Phys. B **1**, 831 (1968); U. Fano, Rep. Prog. Phys. **46**, 97 (1983).
[18] C.-R. Liu, N.-Y. Du, and A.F. Starace, Phys. Rev. A **43**, 5891 (1991).
[19] N.Y. Du, A.F. Starace, and N.A. Cherepkov, Phys. Rev. A **48**, 2413 (1993).
[20] C.D. Lin, Phys. Rev. Lett. **35**, 1150 (1975).
[21] U. Fano, Phys. Rev. A **24**, 619 (1981).
[22] D.A. Harmin, Phys. Rev. A **26**, 2656 (1982).
[23] C.H. Greene, Phys. Rev. A **36**, 4236 (1987).
[24] H.Y. Wong, A.R.P. Rau, and C.H. Greene, Phys. Rev. A **37**, 2393 (1988).
[25] M. LeDourneuf and R.K. Nesbet, J. Phys. B **9**, L241 (1976).
[26] I.I. Fabrikant (unpublished).
[27] M. Gailitis and R. Damburg, Proc. Phys. Soc. London **82**, 192 (1963).
[28] M. Halka, H.C. Bryant, C. Johnstone, B. Marchini, W. Miller, A.H. Mohagheghi, C.Y. Tang, K.B. Butterfield, D.A. Clark, S. Cohen, J.B. Donahue, P.A.M. Gram, R.W. Hamm, A. Hsu, D.W. MacArthur, E.P. MacKerrow, C.R. Quick, J. Tiee, and K. Rozsa, Phys. Rev. A **46**, 6942 (1992).
[29] J.T. Broad and W.P. Reinhardt. Phys. Rev. A **14**, 2159 (1976).
[30] H.A. Hyman, V.L. Jacobs, and P.G. Burke, J. Phys. B **5**, 2282 (1972).
[31] U. Fano, Phys. Rev. **124**, 1866 (1961); U. Fano and J.W. Cooper, *ibid.* **137**, A1364 (1965).
[32] See, e.g., A.F. Starace, Phys. Rev. A **16**, 231 (1977).
[33] Yu.N. Demkov and G.F. Drukarev, Zh. Eksp. Teor. Fiz. **47**, 918 (1964) [Sov. Phys. JETP **20**, 614 (1965)].
[34] *Handbook of Mathematical Functions*, edited by M. Abramowitz and I.A. Stegun (Dover Publications, New York, 1972).
[35] C.-R. Liu and A.F. Starace, Phys. Rev. A **40**, 4926 (1989).
[36] D.E. Aspnes, Phys. Rev. **147**, 554 (1966).